Theoretical study of the molecular hydrogen adsorption and dissociation on different Zn(II) active sites of zeolites

Luis A.M.M. Barbosa [a,*], Georgii M. Zhidomirov [b] and Rutger A. van Santen [a]

[a] *Schuit Institute of Catalysis, Eindhoven University of Technology, PO Box 513, 5600 MB Eindhoven, The Netherlands*
[b] *Boreskov Institute of Catalysis, Prospect Akademika Lavrentieva 5, Novosibirsk 630090, Russia*

Received 24 April 2001; accepted 1 August 2001

The adsorption and dissociation of hydrogen on Zn-exchanged zeolites has been studied theoretically by density functional theory (DFT). Diverse types of active sites have been employed for the Zn cation, such as: placed on different rings (4T and 5T), in the $(ZnO)_4$ (in a cubic configuration cluster) and in the $[Zn–O–Zn]^{2+}$ dimer complex. The Zn(II) cation is most exposed to probe molecules when situated on 4T ring of zeolites. In this position, the cation activates the infrared stretching band of the hydrogen molecule, which is not observed when Zn(II) sits on 5T rings. The assignment of the band shifts found in the experimental IR spectra of hydrogen adsorption, which were associated to the cation position in the zeolite framework, had to be revised following the results for the calculated shifts. Larger shifts are associated to the cationic position at small rings. In the case for $(ZnO)_4$ the dissociative adsorption is more favorable. The calculated activation energy is the lowest among all sites studied. The results have also confirmed the current proposal that ZnO microparticles are responsible for the large H–H stretching shift and the H_2 dissociation on Zn(II) sites in zeolites.

KEY WORDS: adsorption of dihydrogen; DFT calculations; Zn-zeolite

1. Introduction

Zeolite catalysts are extensively used in petroleum refining, as well as in the petrochemical and chemical industries. Recently, a number of new processes have been developed, which are based on metal-loaded zeolites. For instance, Zn zeolites have been used to promote dehydrogenation and aromatization of alkanes, which are well addressed in the literature [1–4].

The catalytic activity of the Zn(II) cation has been subject of a large number of studies [2,3,5–7]. The adsorption of small molecules, especially molecular hydrogen, in combination with vibrational spectroscopy has been widely used to provide information on the adsorption mechanism [8–15]. Nevertheless, a better picture of the Zn(II) cation activity, at certain position inside the zeolites, is still needed.

The present work presents systematically some insights into the hydrogen adsorption on Zn-loaded zeolites. Applying *ab initio* DFT studies at a molecular level, the infrared frequencies, the interaction and activation energies for the hydrogen adsorption on different active sites have been calculated and discussed.

2. Methods

Various active sites for Zn cations are studied for the molecular and dissociative adsorption of the dihydrogen molecule: $[Zn–O–Zn]^{2+}$, $(ZnO)_4$ and Zn^{2+} on different zeolite "fragments" (4T and 5T rings). The $[Zn–O–Zn]^{2+}$ site was studied in combination with a different zeolite fragment: 5T cluster. The $(ZnO)_4$ model, however, was used without direct interaction with the zeolite framework, see figure 1 (a) and (b).

H termination of Si and Al groups has been chosen instead of OH termination to avoid problems such as intramolecular hydrogen bond formation, which results in the creation of a non-acceptable model [16]. Clusters provide qualitatively interesting results for the local interaction between the active site and the probe molecule. The use of such clusters has been extensively discussed elsewhere [17–20].

The $(ZnO)_4$ cubic structure has been chosen as a model in order to mimic one of the different forms of ZnO clusters encapsulated in zeolites [21,22]. This configuration was studied previously by Han *et al.* [23] using grand canonical Monte Carlo simulations in the β-cage of zeolite Y and by the authors for the methane adsorption [24], providing interesting results.

The choice of the basis set took into account the computational needs with the use of extended models for frequency and transition state calculations. All calculations, therefore, have been performed using the following basis set combination: D95-Dunning/Huzinaga full double-ζ for Al and Si atoms [25], double-ζ type plus polarization functions for Zn [26] and triple-ζ type plus polarization functions for H and O, as implemented in Gaussian 98 [27].

The B3LYP functional was used, since it gives acceptable values for molecular vibrations [28], energies and geome-

---

[*] To whom correspondence should be addressed. Present address: Institut de Recherches sur la Catalyse (IRC), Centre National de La Recherche Scientifique (CNRS), 2, Av. Albert Einstein, Villeurbanne Cedex, France. E-mail: lbarbosa@catalyse.univ-lyon1.fr

1011-372X/01/1100-0055$19.50/0

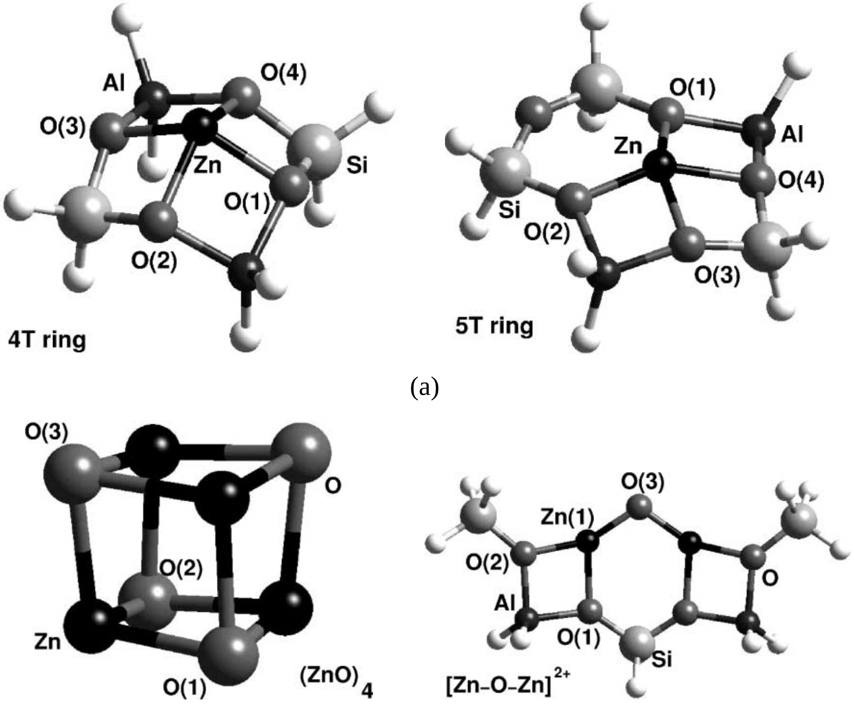

(a)

(b)

Figure 1. Zn(II) site models: (a) the zeolite rings, (b) $(ZnO)_4$ and $[Zn–O–Zn]^{2+}$.

tries [29–31]. Furthermore, this functional also has been recently used to study proton donation [32], weak and strong H bonds [33–35] with reliable results.

All the stationary points were verified by frequency calculations. These tests produce either no imaginary frequencies, which is required for local minimum, or just one, which is characteristic for transition states [36].

All frequencies used for the this study were scaled by 0.96, as suggested previously by Pople *et al.* [31] and Radom *et al.* [37]. Although Gaussian 98 [27] evaluates only the harmonic vibration frequencies, the comparison of such values with experimental results showed to be very useful in the analysis of the induced changes in the IR spectra of the adsorbed probe molecules, for instance in the study of the methane interaction cations exchanged in zeolites [24,38].

The basis set superposition error (BSSE) was verified using a counterpoise (CP) method [39]. The two-body method was applied in all molecular adsorption cases and this correction was included in all energy values, when needed. No symmetry constraints have been used for the configurations studied.

3. Results and discussion

The results will be divided in different parts. In the first one, the interaction of the molecular hydrogen with two distinct Zn^{2+} cation positions is analyzed. In the second part the same study is followed for two other sites for the Zn(II) cation in zeolites. In the last part the dissociation path of the molecular hydrogen is discussed for all cases.

3.1. H_2 as a probe for the Zn(II) siting

Two different positions of Zn^{2+} are analyzed in this part: 4T and 5T rings. The four-membered ring is found in several zeolites, for instance faujasites and zeolite A. This position corresponds to the S_{III} and $S_{III'}$ sites in these zeolites. The second model represents the cation position in the other two types of rings found in zeolites (5- and 6-membered rings), commonly in ferrierite, ZSM-5 and faujasites.

The zinc cation is out of the plane of the oxygen atoms in the 4T ring model (see figure 1(a)), as it has been already mentioned in several different works [2,5,7,24,40]. The cation sits in a tetra-coordinated configuration, in which the Zn–O distances are all equal to 2.00 Å, see table 1.

In the 5T ring, the Zn(II) cation sits in the plane of the oxygen atoms, see figure 1(a). This relative position of the cation can, however, be modified by using different descriptions for the ring model [5,6]. If the atoms that form the ring are frozen in their experimental position, the cation position is shown to be slightly out of the plane of the oxygen atoms. Therefore, the cationic position depends on the flexibility of the ring, as suggested previously by the authors [41].

The oxygen atoms of the zeolite framework screen the cation charge, decreasing its polarizing power. The strength of this screening effect depends on the spatial arrangement of these atoms. For this reason, one may expect that the Zn(II) in the “real” 5-membered ring may be slightly more

Table 1
The calculated distances of different Zn(II) systems, values in Å.

	Zn–O				Zn–H		O(3)–H(b)
	O(1)	O(2)	O(3)	O(4)	H(a)	H(b)	
4T ring							
Active site	2.00	2.00	2.00	2.00	–	–	–
Adsorption complex	2.03	2.02	2.03	2.02	2.16	2.16	3.39
Transition state	2.01	2.02	2.54	2.02	1.74	1.91	1.35
Dissociative complex	2.12	2.09	2.10	2.10	1.54	–	0.96
5T ring							
Active site	1.94	2.05	2.05	3.11	–	–	–
Adsorption complex	1.94	2.06	2.06	3.12	2.69	2.69	3.61
Dissociative complex	2.02	2.09	3.19	2.06	1.55	–	0.96
$[Zn–O–Zn]^{2+}$ (for Zn(1))							
Active site	2.02	1.90	1.77		–	–	–
Adsorption complex	2.02	1.90	1.78		–	3.57	–
Transition state	2.00	1.93	1.94		1.90	1.87	–
Dissociative complex	2.01	1.97	1.93		1.74	–	0.96
$(ZnO)_4$							
Active site	1.97	1.97	1.97		–	–	–
Adsorption complex (Zn site)	1.98	1.98	1.98		2.12	2.13	3.44
Adsorption complex (O site)	1.98	1.98	1.98		3.90	–	2.31
Transition state	1.94	1.94	2.27		1.86	1.86	1.56
Dissociative complex	1.98	1.98	3.61		1.53	–	0.95

Table 2
The calculated results for the adsorption of the dihydrogen molecule.

System	Adsorption energy ($kJ\,mol^{-1}$)	Adsorption energy + Zpe + BSSE ($kJ\,mol^{-1}$)	Frequency, $\Delta\nu$ (cm^{-1})	d(H–H) (Å)
H_2	–	–	0	0.742
$(ZnO)_4$ (Zn)	−9.95	+1.53	−174	0.753
$(ZnO)_4$ (O)	−5.68	+3.05	−113	0.747
4T ring	−14.6	−1.70	−157	0.752
5T ring	−2.74	+8.27	−54	0.745
$[Zn–O–Zn]^{2+}$	−4.86	+3.46	−99	0.746

active than the one at full optimized structure and that the molecular hydrogen will interact stronger with the cation at the 4-membered than at the 5-membered ring. Hence, the hydrogen has been used as a probe for the distinct structural cationic position experimentally [11,42].

The comparison of the adsorption energy, H–H bond distance and shift of the H–H stretching frequency draws a complete picture of the relative strength of the interaction between H_2 and the cation.

For instance, the H–H stretching frequency has a large shift when the H_2 interacts with the more exposed Zn(II), see table 2. The shift calculated at the 4T ring position is about three times larger than at the 5T ring.

In a recent work, Kazansky *et al.* [14] probed ZnNaY zeolites with H_2, and a large shift ($\Delta\nu = -123$ cm^{-1}) was obtained for the stretching vibration of the H–H bond. This shift only occurred when Zn(II) was exchanged on the original NaY zeolite, therefore this band was assigned to Zn(II) at the position S_{II}, which corresponds to the 6-ring window in the supercage. This value is larger than the one obtained for the adsorption of H_2 on the 5-membered ring but similar to the one obtained at the 4-membered ring position (S_{III}), see table 2.

Seidel *et al.* [43] have also studied ZnNaY catalysts, which have been prepared by solid-state ion exchange. Both S_{II} and S_{III} cationic positions are occupied at high overall cation exchange. Furthermore, in the samples obtained by wet exchange the concentration of Zn(II) ions in the S_{III} position exhibits a similar behavior. Seff *et al.* [44] have modified completely two different NaX zeolite crystals, one partially dehydrated and the other fully hydrated, by wet exchange of $Zn(NO_3)_2$. In both cases, one of the most populated sites for the Zn cation is the S_{III}. Therefore, one may conclude that this large shift ($\Delta\nu = -123$ cm^{-1}) is better assigned to the H_2 adsorption close to the 4-membered ring in the supercage.

In respect to the relative position of the H_2 molecule to the Zn cation, both sites show the same feature: the molecule interacts with the active site similarly to an η^2 bonded complex, see figure 2(a). The Zn–H distances are shorter for the case of the 4T ring. One may also notice that in the latter case, the Zn–O distances increased by 0.02 Å, see table 1. In the 5-membered ring case there were no changes in these distances upon the H_2 adsorption. These results confirm the weak interaction between the molecule and the Zn(II) cation in the 5T ring.

Similar adsorption configuration has been reported for the molecular hydrogen complexes with transition metals [45–48], which is called a non-classical configuration for the transition-metal hydride. The H–H distance for this non-classical geometry has its value within 0.8–1.12 Å in several complexes [46,47].

The calculated value for the H–H bond length of the H_2 molecule adsorbed at the 4T ring is slightly shorter than the

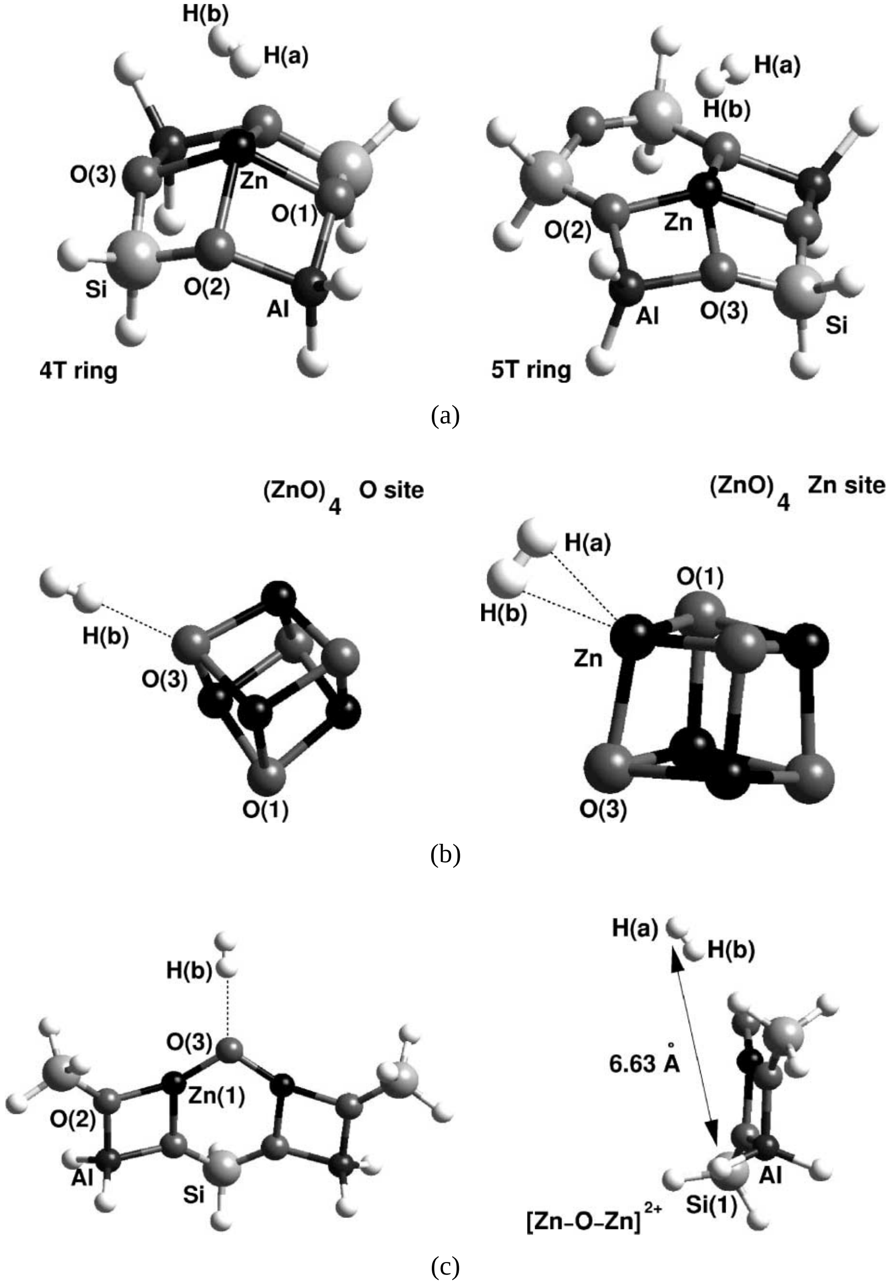

Figure 2. Molecular adsorption of H_2 on the Zn(II) site models: (a) the zeolite rings, (b) the $(ZnO)_4$ models, (c) the $[Zn–O–Zn]^{2+}$.

previous range. Nevertheless, one may notice that the H–H bond has been already stretched by 0.01 Å (see table 2) from the gas phase configuration, which confirms the interaction with the cation.

This different stretching value can be explained by the separation between the probe molecule and the cation, which is large enough to prevent the interaction of the H_2 (σ) bonding electrons with the empty orbital of the cation and the metal d electrons to engage in a back donation, which weakens the H–H bond [46].

Interaction of H_2 with distinct cationic sites

The low Al content found in several zeolites suggests that two Al atoms may not sit in the same neighborhood. Therefore, different models from the Zn(II) cation [3,7,49] have been proposed for the active form of zinc in such zeolites: $Zn(OH)^+$ [40,50,51], $[Zn–O–Zn]^{2+}$ [3] and, more recently, associated to ZnO microparticles [14,15].

In order to analyze the interaction between the H_2 molecule with the ZnO microparticles, a $(ZnO)_4$ model was used, see figure 1(b). The stability of this model has been calculated by comparing the required energy to form the Zn(II) sites, at the 5T ring position [24]. The stability was shown to depend on the size of the microparticles, which has been recently confirmed by experimental studies [21,22].

This model has an exposed Zn(II) cation, which interacts with the probe molecule similarly to the 4-membered ring position. Both values found for the shift of the H–H stretching frequency and the change in the H–H bond length are in agreement, see table 2.

Kazansky *et al.* [10,14,15] have shown for Zn-containing ZSM5 that hydrogen IR spectra demonstrated a strong perturbation of the symmetric stretching vibration mode upon adsorption: about $-208\ \mathrm{cm}^{-1}$ for the 3ZnO/HZSM5 zeolites [10] and $-223\ \mathrm{cm}^{-1}$ for Zn/HZSM5 prepared by incipient wetness impregnation. Such strong perturbation was assigned to the interaction with Lewis-base pairs on the surface of nanometric clusters. The calculated shift was $\Delta\nu = -174\ \mathrm{cm}^{-1}$ for the hydrogen interaction with Zn(II), which is closer to these experimental values. Therefore, it is possible to conclude that indeed this large shift is caused by the ZnO nanoparticles.

The H_2 molecule also binds in the η^2 type configuration, see figure 2(b). The Zn–H distances are slightly shorter than those previously found for the Zn(II) at the 4T ring, see table 1. The Zn–O distance, however, does not show any perturbation after the interaction with the probe molecule.

The H–H bond suffers similar stretching as seen previously for the adsorption at the 4-membered ring position. The optimized bond length is smaller than the value of 0.8 Å (the lowest value for the H–H distance in the non-classical configuration), which is again due to separation between probe molecule and the Zn(II) cation.

It is well known that standard quantum chemical calculations usually give exaggerated values of the binding energies of weakly bonded complexes due to the finite basis set approximation [39]. To prevent this overestimation, the BSSE correction has been applied. One may observe in table 2 that the same trend is observed for the adsorption energy values (corrected or not) and for the shifts of the H–H stretching frequency. Two points should be noticed here, the positive values for the corrected adsorption energies and the large shift calculated for the case of the $(ZnO)_4$ model. These results may be explained by the very small value for the interaction energy that the H_2 molecule has with all studied sites, which are within the accuracy of the calculations, and by the overestimation of the BSSE correction that the CP method usually provides [52]. No improvement has been obtained when these systems were recalculated using the more expensive MP2 method.

In addition, the H_2 molecule can interact with the oxygen atoms, which are more exposed than the ones from the framework, see figure 2(b). The final configuration is different from the one found previously. The H_2 is adsorbed by following the end-on mode. This adsorption is weaker than the one found for the Zn(II) site, see table 2. Therefore, this indicates that the H_2 will adsorb preferentially on the Zn cation of the ZnO microparticles.

The other model studied is the $[\mathrm{Zn–O–Zn}]^{2+}$ site, which is represented here interacting with a 5T cluster model (see figure 1(b)). This 5T cluster represents part of the large rings of zeolites, for instance, the 10-membered ring of ZSM5. Shubin *et al.* [6] also used this active site for calculations but between two different 5T rings of ZSM5. The $[\mathrm{Zn–O–Zn}]^{2+}$ site was shown to be more stable than the $(ZnO)_4$ microparticle [24].

The optimized structure of this model is symmetric and remains in this way after increasing the size of the cluster model up to a 8-membered ring [24]. This site does not have an exposed Zn(II) cation, therefore one could expect weaker interaction with the H_2.

Interestingly, the probe molecule interacts with the bridge oxygen from this site, in a similar way to the oxygen atom of the $(ZnO)_4$ model, see figure 2(c). Both positions induce similar IR shifts and H–H bond stretching in the H_2 molecule (see table 2), which leads to the conclusion that H_2, indeed, interacts weakly with both sites.

The distance between the Si atom (Si(1)) of the 5T cluster, which represents the zeolite framework, and the H(a) of the H_2 molecule is very large, about 6.63 Å see figure 2(c). If one considers the dimensions of the ZSM5 pore (5.3 × 5.6 Å), it is possible to suggest that the probe molecule will suffer some steric constraints from the zeolite framework upon adsorption on this site.

3.2. Dissociation of H_2

The dissociative adsorption of hydrogen was also studied for all sites, see figure 3 (a) and (b). The transition state and the activation energy, however, have been calculated only for the sites with which the H_2 molecule has strong interaction, see figure 4 (a) and (b).

One may note in table 3 that the dissociation energy has only a positive value for the 5-membered ring case, which confirms that the Zn(II) at this position does not activate the H_2 molecule. This result is in complete agreement with the experimental evidence, which indicates that the Zn^{2+} cation located at the 6-membered ring of zeolite Y does not dissociate this molecule at room temperature nor at elevated temperatures up to 573 K [15].

In the case of the 4-membered ring, this energy value is negative, which indicates that the product of the dissociation is more stable. On the other hand, there is a slight high activation energy, which indicates that this dissociation is activated.

Moreover, there is an active participation of the oxygen atom of the framework during this dissociation, see the distance O(3)–H(b) in table 1. This is in very good agreement with the recent studies of the adsorption of H_2 on Ag^+-exchanged zeolites A and Y [53].

Frash *et al.* [2] had calculated the activation energy of the inverse reaction in their study of alkyl activation of ethane by Zn(II) cations in zeolites. They also used the 4T ring as a model for the active site and the activation energy value found was in good agreement with the value calculated here.

The dissociation of the H_2 molecule on Zn(II) may be an interesting alternative for the hydrogenation of hydrocarbons. Such process has been studied by different groups [54–56] for Na^+ zeolites. In [54] the first step for such reaction was suggested as the heterolytic dissociative

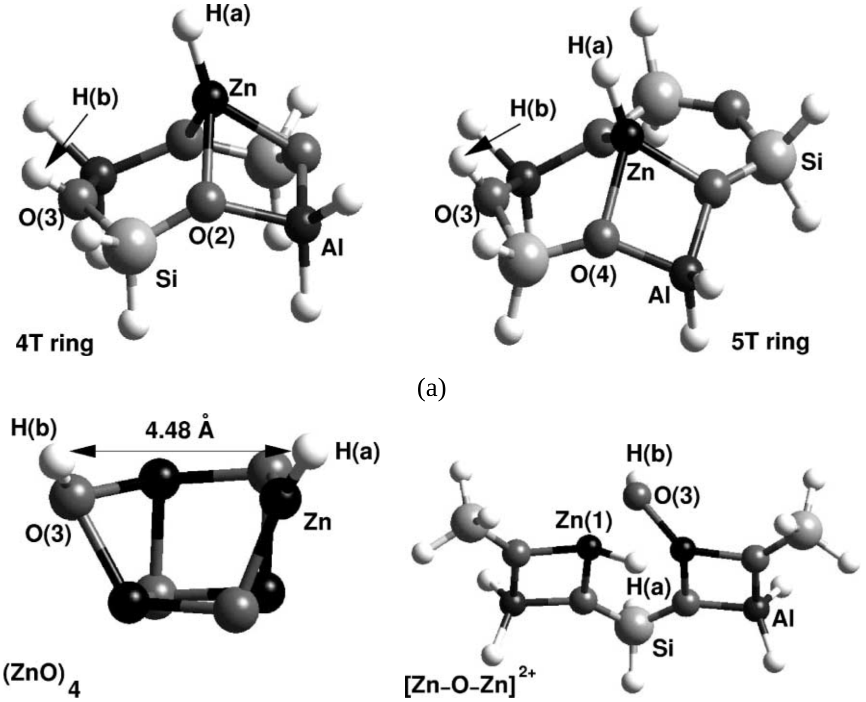

(a)

(b)

Figure 3. Dissociative adsorption of H_2 on the Zn(II) site models: (a) the zeolite rings, (b) $(ZnO)_4$ and $[Zn–O–Zn]^{2+}$.

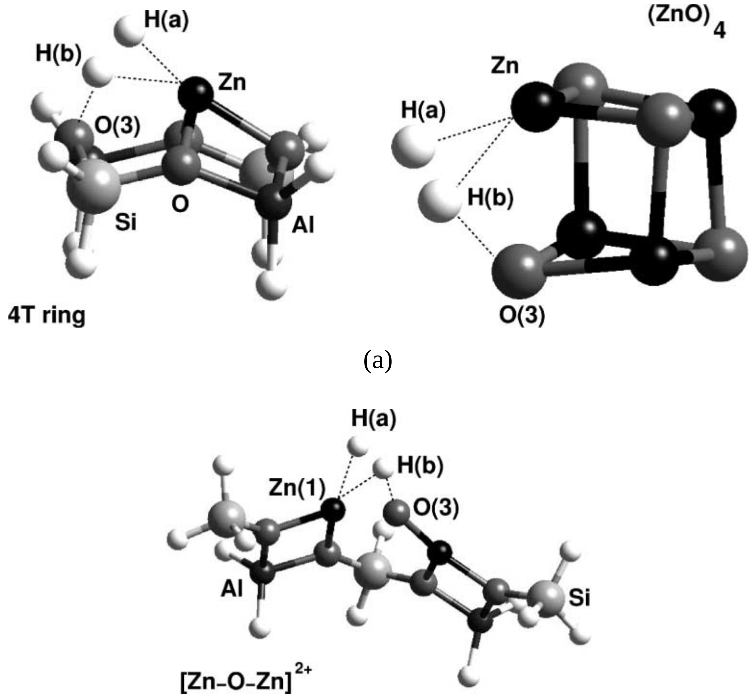

(a)

(b)

Figure 4. Transition state of the H_2 dissociation on the Zn(II) site models: (a) the 4T ring and $(ZnO)_4$, (b) $[Zn–O–Zn]^{2+}$.

adsorption of the hydrogen molecule, which agrees with the latter proposal.

Regardless of the adsorption mode (on the Zn(II) cation or the oxygen atom) in the case of the $(ZnO)_4$ model, the dissociation energy has a large negative value, see table 3. In the same way, the activation energy is the lowest calculated in this work. Therefore, one may conclude that the H_2, most likely, will prefer to dissociate in such sites.

The value of the dissociation energy may be slightly lower than the one shown in table 3 due to possible geometric

Table 3
The dissociation energies of the dihydrogen molecule.

System	Dissociation energy + Zpe ($\mathrm{kJ\,mol^{-1}}$)	Activation energy + Zpe ($\mathrm{kJ\,mol^{-1}}$)
$(ZnO)_4$ (Zn)	-140	23
$(ZnO)_4$ (O)	-145	30
4T ring	-11	75
5T ring	$+45$	–
$[Zn–O–Zn]^{2+}$	-60	82

constraints from the zeolite framework. The optimized geometry is an open structure, see figure 3(b). The distance between H(Zn–H) and H(OH group) is 4.48 Å, which is slightly smaller than the pore diameter of the ZSM5 (5.3 × 5.6 Å).

The oxygen atom has also an active role in the dissociation process similarly to the case of the 4T ring, as one may see from the transition state configurations (see figure 4(a)) and the O(3)–H(b) distances (see table 1).

Kazansky *et al.* [10,13,15] have proposed that this site is responsible for the dissociation of H_2 and of other nonpolar molecules like methane. Such site should be related to a form of acid–base Zn^{2+}–O^{2-} pairs. The calculated results are in complete agreement with this suggestion.

The authors have previously shown by theoretical calculations that methane also preferred a dissociative adsorption on such system but the large experimental shift in the C–H stretching frequency upon adsorption was not observed [24].

For the $[Zn–O–Zn]^{2+}$ site, the dissociation process is also favorable but not as for the $(ZnO)_4$ model. The activation energy is the highest calculated here, therefore the dissociation reaction is strongly activated, in a similar way to the 4T ring case.

Similarly to the other cases studied here, the participation of the oxygen atom from the $[Zn–O–Zn]^{2+}$ site is very important. One may compare the O(3)–H(b) distance and the transition state structures, see table 1 and figure 4 (a) and (b).

The symmetric arrangement found in the optimized geometry, see figure 3(b), has been tested previously and remains symmetric regardless of the size of the model [24].

In addition, the stretching frequencies of the ZnH and OH groups formed during the dissociation reaction have been studied, see table 4. The value found for the OH stretching in the $(ZnO)_4$ site is close to the value for the Brønsted site, which was calculated for a 4T cluster model, see table 4 (entry 4T (H^+)). This similarity could lead to a misinterpretation of this band for Zn(II)-exchanged zeolites, produced using ZnO particles. The same occurs to the OH stretching values of the other models. This indicates that such frequency cannot be used as a fingerprint of these Zn(II) sites.

On the other hand, the values of the Zn–H stretching are different enough to discriminate these sites, see table 4. It should be noticed here that the values for the Zn–H stretching found for bulk ZnO [13], 1610 and 1589 cm^{-1}, are smaller than the one found here. This could be understood due the fact that the $(ZnO)_4$ model does not represent the bulk ZnO.

Table 4
The OH and ZnH stretching frequencies for different clusters, values in cm^{-1}.

System	OH stretching	Zn–H stretching
$(ZnO)_4$	3709	1787
4T ring	3681	1809
5T ring	3683	1755
4T (H^+)	3727	–
$[Zn–O–Zn]^{2+}$	3697	1259

4. Conclusions

The adsorption and dissociation of molecular hydrogen on Zn-exchanged zeolites has been studied theoretically by density functional theory (DFT). Diverse types of active sites have been employed for the Zn cation, such as: placed on different rings (4T and 5T), in the $(ZnO)_4$ (in a cubic configuration cluster) and in the $[Zn–O–Zn]^{2+}$ dimer complex.

The Zn(II) cation is most exposed to probe molecules when sitting on the 4T ring of the zeolites. In this position, the cation activates the stretching frequency of the H–H bond. Such activation is not observed when the cation is placed in the 5T ring.

The assignment of some bands shifts found in the experimental IR spectra of hydrogen adsorption, which were associated to the cation position in the zeolite framework, had to be revised following the results for the calculated shifts. Larger shifts are associated with the cationic position at small rings.

Hydrogen prefers to adsorb physically on Zn(II) at 4T rings. Its dissociative process requires an activation energy of 56 $\mathrm{kJ\ mol^{-1}}$. This is not the case for the $(ZnO)_4$ model, for which dissociative adsorption is more favorable.

The $[Zn–O–Zn]^{2+}$ site is thermodynamically more stable than the $(ZnO)_4$ structure. However, the hydrogen interacts weakly with the former model, having the highest activation energy for dissociation.

The calculations confirmed the experimental proposal [10,13–15] that the ZnO microparticles loaded in zeolites are responsible for the large shift found for the H–H stretching frequency and the H_2 dissociation.

Acknowledgement

The authors thank Professor Dr. Vladimir B. Kazansky for very useful discussions. GMZ thanks the financial support from Dutch Science Foundation in the collaborative Russian–Dutch research projects and LAMMB the National Council of Scientific and Technologic Development (CNPq, Brazil) and Eindhoven University of Technology (TUE, The Netherlands).

References

[1] Y. Ono, Catal. Rev. Sci. Eng. 34 (1992) 179.
[2] M.V. Frash and R.A. van Santen, Phys. Chem. Chem. Phys. 2 (2000) 1085.
[3] J.A. Biscardi, G.D. Meitzner and E. Iglesia, J. Catal. 179 (1998) 192.
[4] N. Kumar and L.-E. Lindfors, Catal. Lett. 38 (1996) 239.
[5] A.A. Shubin, G.M. Zhidomirov, A.L. Yakovlev and R.A. van Santen, J. Phys. Chem B 105 (2001) 4928.
[6] A.A. Shubin, G.M. Zhidomirov, A.L. Yakovlev and R.A. van Santen, Catal. Lett. 70 (2000) 175.
[7] L.A.M.M. Barbosa and R.A. van Santen, Catal. Lett. 63 (1999) 97.
[8] A.V. Larin and E. Cohen de Lara, J. Chem. Phys. 101 (1994) 8130.
[9] A.V. Larin and E. Cohen de Lara, Mol. Phys. 88 (1996) 1399.
[10] V.B. Kazansky, L.M. Kustov and A.Y. Khodakov, in: *Zeolites: Facts, Figures, Future*, eds. P.A. Jacobs and R.A. van Santen (Elsevier, Amsterdam, 1989) p. 1173.
[11] L.M. Kustov and V.B. Kazansky, J. Chem. Soc. Faraday Trans. 87 (1991) 2675.
[12] A.Y. Khodakov, L.M. Kustov, V.B. Kazansky and C. Williams, J. Chem. Soc. Faraday Trans. 89 (1993) 1393.
[13] E.B. Uvarova, L.M. Kustov, I.I. Lishchiner, O.V. Malova and V.B. Kazansky, in: *Studies in Surface Science and Catalysis*, Vol. 105, eds. H. Chon, S.-K. Ihm and Y.S. Uh (Elsevier, Amsterdam, 1997) p. 1243.
[14] V.B. Kazansky, V.Y. Borovkov, A.I. Serykh, R.A. van Santen and P.J. Stobbelaar, Phys. Chem. Chem. Phys. 1 (1999) 2881.
[15] V.B. Kazansky, V.Y. Borovkov, A.I. Serykh, R.A. van Santen and B.G. Anderson, Catal. Lett. 66 (2000) 39.
[16] J. Sauer, P. Ugliengo, E. Garrone and V.R. Saunders, Chem. Rev. 94 (1994) 2095.
[17] G.J. Kramer, A.J.M. de Man and R.A. van Santen, J. Am. Chem. Soc. 113 (1991) 6435.
[18] J.D. Gale, Topics Catal. 3 (1996) 169.
[19] R. Shah, J.D. Gale and M.C. Payne, J. Phys. Chem. B 101 (1997) 4787.
[20] V.V. Mihaleva, R.A. van Santen and A.P.J. Jansen, J. Chem. Phys., accepted for publication.
[21] J.E. Readman, I. Gameson, J.A. Hrijac, P.P. Edwards and P.A. Anderson, Chem. Commun. (2000) 595.
[22] H.B. Lee, H.M. Lim and C.S. Han, Bull. Korean Chem. Soc. 19 (1998) 1002.
[23] H.M. Lim and C.S. Han, Bull. Korean Chem. Soc. 20 (1999) 143.
[24] L.A.M.M. Barbosa, G.M. Zhidomirov and R.A. van Santen, Phys. Chem. Chem. Phys. 2 (2000) 3909.
[25] T.H. Dunning Jr. and P.J. Hay, in: *Modern Theoretical Chemistry*, ed. H.F. Schaefer III (Plenum, New York, 1976) p. 1.
[26] V. Rassolov, J.A. Pople, M. Ratner and T.L. Winder, J. Chem. Phys. 109 (1998) 1223.
[27] M.J. Frisch, G.W. Trucks, H.B. Schlegel, G.E. Scuseria, M.A. Robb, J.R. Cheeseman, V.G. Zakrzewski, J.A. Montgomery Jr., R.E. Stratmann, J.C. Burant, S. Dapprich, J.M. Millam, A.D. Daniels, K.N. Kudin, M.C. Strain, O. Farkas, J. Tomasi, V. Barone, M. Cossi, R. Cammi, B. Mennucci, C. Pomelli, C. Adamo, S. Clifford, J. Ochterski, G.A. Petersson, P.Y. Ayala, Q. Cui, K. Morokuma, D.K. Malick, A.D. Rabuck, K. Raghavachari, J.B. Foresman, J. Cioslowski, J.V. Ortiz, B.B. Stefanov, G. Liu, A. Liashenko, P. Piskorz, I. Komaromi, R. Gomperts, R.L. Martin, D.J. Fox, T. Keith, M.A. Al-Laham, C.Y. Peng, A. Nanayakkara, C. Gonzalez, M. Challacombe, P.M.W. Gill, B. Johnson, W. Chen, M.W. Wong, J.L. Andres, C. Gonzalez, M. Head-Gordon, E.S. Replogle and J.A. Pople, Gaussian 98, Revision A.5 (Gaussian, Pittsburgh, PA, 1998).
[28] R.A. van Santen, Catal. Today 38 (1997) 377.
[29] J.B. Nicholas, Topics Catal. 4 (1997) 157.
[30] W. Koch and R.H. Hertwig, Chem. Phys. Lett. 286 (1997) 345.
[31] L.A. Curtiss, K. Raghavachari, P.C. Redfern and J.A. Pople, Chem. Phys. Lett. 270 (1997) 419.
[32] D.M. Smith, B.T. Golding and L. Radom, J. Am. Chem. Soc. 121 (1999) 9388.
[33] A.K. Chandra and M.T. Nguyen, Chem. Phys. 232 (1998) 299.
[34] J.B. Nicholas, Topics Catal. 9 (1999) 181.
[35] R. Arnaud, C. Adamo, M. Cossi, A. Millet, Y. Vallé and V. Barone, J. Am. Chem. Soc. 122 (2000) 324.
[36] H. B. Schlegel, in: *Ab initio Methods in Quantum Chemistry-I*, ed. K. P. Lawley (Wiley, New York, 1987) p. 249.
[37] A.P. Scott and L. Radom, J. Chem. Phys. 100 (1996) 16502.
[38] A.M. Ferrari, K.M. Neyman, S. Huber, H. Knözinger and N. Rösch, Langmuir 14 (1998) 5559.
[39] G. Lendvay and I. Mayer, Chem. Phys. Lett. 297 (1998) 365.
[40] L.A.M.M. Barbosa and R.A. van Santen, J. Mol. Catal. A 166 (2001) 101.
[41] L.A.M.M. Barbosa, R.A. van Santen and J. Hafner, J. Am. Chem. Soc. 123 (2001) 4530.
[42] J. Eckert, J.M. Nicol, J. Howard and F.R. Trouw, J. Phys. Chem. 100 (1996) 10646.
[43] A. Seidel, G. Kampf, A. Schmidt and B. Boddenberg, Catal. Lett. 51 (1998) 213.
[44] D. Bae and K. Seff, Micropor. Mesopor. Mater. 40 (2000) 233.
[45] G.J. Kubas, R.R. Ryan, B.I. Swanson, P.J. Vergamini and H.J. Wasserman, J. Am. Chem. Soc. 106 (1984) 451.
[46] D.G. Hamilton and R.H. Crabtree, J. Am. Chem. Soc. 110 (1988) 4126.
[47] L.S. van der Sluys, J. Eckert, O. Eisenstein, J.H. Hall, J.C. Huffman, S.A. Jackson, T.F. Koetzle, G.J. Kubas, P.J. Vergamini and K.G. Caulton, J. Am. Chem. Soc. 112 (1990) 4831.
[48] W.D. Harman and H. Taube, J. Am. Chem. Soc. 112 (1990) 2261.
[49] El-M. El-Malki, R.A. van Santen and W.M.H. Sachtler, J. Phys. Chem. B 103 (1999) 4611.
[50] E. Iglesia, J.E. Baumgartner and G.L. Price, J. Catal. 134 (1992) 549.
[51] S. Valange, Z. Gabelica, B. Onida and E. Garrone, in: *12th Int. Zeolite Conference*, eds. M.M. Treacy, B.K. Markus, M.E. Bisher and J.B. Higgins (Baltimore, MD, 1999) p. 2711.
[52] B. Paiz and S. Suhai, J. Comp. Chem. 19 (1998) 575.
[53] T. Baba, N. Komatsu, H. Sawada, Y. Yamaguchi, T. Takahashi, H. Sugisawa and Y. Ono, Langmuir 15 (1999) 7894.
[54] Kh.M. Minachev, V.I. Garanin, V.V. Kharlamov and T.A. Isakova, Kinet. Katal. 13 (1972) 1101.
[55] J. Kanai, J.A. Martens and P.A. Jacobs, J. Catal. 133 (1992) 527.
[56] S. Senger and L. Radom, J. Am. Chem. Soc. 122 (2000) 2613.